

# Static Fire Test Stand for Jet Vanes Analysis

Shalini Shailesh\*, Margaret Hwang\*, Catherine Fang\*, Alexander Swift\*, Ahmet Baturay Coksaygili\*, Kush Bandi\*, Owen Pollack\*, Pritham Sathish\*

*Georgia Institute of Technology, Atlanta, Georgia, 30332, United States*

**Experimental solid rocket programs involve testing to confirm the viability of structures, propulsion, and electronics. Motor test stands are a useful tool for large-scale rockets to measure the thrust forces and generate a previously unknown thrust curve. The GNC Project within the Ramblin' Rocket Club at Georgia Tech has built a test stand to gather load data, evaluate thermal properties of various materials, and prepare for a controlled test of a jet vanes rocket. Jet vanes, which are fin deflectors located in the exhaust of a rocket's nozzle, are used to control the flight path of a rocket. The vanes are subject to high temperatures, supersonic turbulent conditions, and erosion from precipitates escaping the combustion chamber, resulting in the engineering challenge of finding a material that can resist these extreme conditions and perform the necessary deflections to allow controlled flow. A test-stand is required to test candidate materials. This paper describes the challenges, constraints, designs, and analysis of the first such static fire conducted by the GNC Project, and the procedures followed to ensure structural stability, ease of manufacturing, and safety. Furthermore, this paper will outline the final material selection for the jet vanes and the reasons for doing so.**

## I. Introduction and Background

Thrust Vector Control (TVC) is a method used in rocketry to manipulate the direction of thrust produced by the rocket engine. The goal of this project is to enhance maneuverability, allowing rockets to change orientation, and adjust their flight path. TVC systems involve various systems such as gimbals or vanes to achieve precise control over thrust direction. In essence, TVC enables rockets to navigate and accomplish missions with greater precision and efficiency than thrust direction that is not manipulated. The final goal of the project by the GNC team is to apply ideas learned through testing towards an actively stabilizing rocket.

The research presented in this paper focuses on two primary objectives: evaluating the thrust loss percentage when jet vanes remain stationary and identifying erosion-resistant materials during burn time. This current paper is based off a test stand designed for a 54mm motor with still vanes. Using this data, two more upcoming tests will be performed using a 98mm motor where the jet vanes will be moving. Tests using the 98mm motor test stand aim to gather empirical data on the thrust vector control (TVC) effectiveness by dynamically adjusting the positions of the jet vanes.

Jet vane thrust vector control (JTVTC) systems are the main design used in this project which operate by deflecting small fins in the rocket's exhaust at various angles of attack to redirect the flow and create moments on the vehicle [3]. By adjusting the angle of the vanes, the thrust can be redirected in any desired direction, allowing for controlled attitude. A drawback of jet vanes is the thrust loss due to drag caused by their presence in the exhaust, typically resulting in a thrust loss percentage ranging from 1% to 5% depending on the drag coefficient. The data of thrust loss for when the vanes are kept static collected from this test fire will aid in setting expectations for the thrust loss experienced when the vanes' motions is controlled within the next test fire. When considering materials for jet vanes, heat resistance is a critical factor due to the extreme temperatures experienced within the rocket engine exhaust. Graphite, tungsten copper, tungsten carbon, and steel were considered in this investigation due to their favorable properties in high temperature environments. The material demonstrating minimal erosion will be selected for manufacturing the primary jet vanes for the next test fires. This standardization process ensures optimal performance

1 Undergraduate Member, GT Ramblin' Rocket Club, Daniel Guggenheim School of Aerospace Engineering, AIAA Student Member 1603240  
2 Undergraduate Member, GT Ramblin' Rocket Club, Daniel Guggenheim School of Aerospace Engineering, AIAA Student Member 1603466  
3 Undergraduate Member, GT Ramblin' Rocket Club, Daniel Guggenheim School of Aerospace Engineering, AIAA Student Member 1603551  
4 Undergraduate Member, GT Ramblin' Rocket Club, Daniel Guggenheim School of Aerospace Engineering, AIAA Student Member 1405486  
5 Undergraduate Member, GT Ramblin' Rocket Club, Daniel Guggenheim School of Aerospace Engineering, AIAA Student Member 1603093  
6 Undergraduate Member, GT Ramblin' Rocket Club, Daniel Guggenheim School of Aerospace Engineering, AIAA Student Member 1603262  
7 Undergraduate Member, GT Ramblin' Rocket Club, Daniel Guggenheim School of Aerospace Engineering, AIAA Student Member 1603243  
8 Undergraduate Member, GT Ramblin' Rocket Club, Daniel Guggenheim School of Aerospace Engineering, AIAA Student Member 1603558

and durability of the thrust vectoring mechanism. Ultimately, the data obtained will be instrumental in refining the design and optimization of thrust vectoring mechanisms and selecting materials for the actively stabilized rocket.

## II. Nomenclature

$\alpha$	=	angle of attack
$f$	=	generic function
$H$	=	hardness of the abraded material
$H_a$	=	hardness of the abrading material
$k$	=	microstructural parameter
$K$	=	erosion as percent mass.
$\lambda$	=	sharpness Factor
$n$	=	number of particles
$\Omega$	=	toughness
$\phi$	=	material cutting energy

## III. Methods and Design

### A. Test Stand Frame & Structural Integrity

The test stand was designed based on 3 criteria: structural integrity, data acquisition accuracy, and cost. With all these criteria, the design was finalized.

The first major requirement was structural integrity. The team went with a design that has an upward facing thrust vector. In addition, rather than using ball transfers, which cannot serve as a structural restriction for diagonal deviations, a force transfer ring was developed. There were also temperature-related considerations made to determine what materials would be used. Steel and other materials with relatively high melting temperatures were used, particularly for sections subjected to significant heat loads.

The second criterion was the data acquisition accuracy of our system. The 54 mm test stand is a smaller test platform for the bigger upcoming 98mm test stand, which requires high accuracy force measurement capabilities to characterize the relationship between thrust vector and jet vane deflection angle. Therefore, with this stand, structural deflections were designed to be minimized. This was achieved through usage of mild steel bars, which have higher stiffness compared to aluminum “T-slot” bars which are commonly used in experimental setups. Three aluminum mounting plates were used to decrease horizontal or vertical deflections. Load cells, connected to the force transfer ring and motor forward closure, and a National Instruments CompactDAQ were used for force measurements.

The final criterion concerned relative cost. The cost of our test materials and the intention to conduct more static fires and tests resulted in budgetary constraints. To address these problems, most of the construction was designed using materials available to our team. The structural backbone of the system was repurposed from used launch structures, and fasteners such as rivets were chosen to reduce production time. Loadcells were purchased from a low-cost offshore manufacturer and calibrated in-house. Overall, these considerations result in a high performance-to-cost test structure suitable for both thrust vectoring and future motor testing applications.

The platform was constructed by making rough band saw cuts for the extrusions, which were then faced and milled down to size. All holes and crucial dimensions were machined with a tolerance of  $\pm 10$  thousands of an inch. The top and bottom plates were cut with a water jet. Most of the structure is built with 2-dimensional plates in mind due to relative ease of manufacturing using the methods available to us. Cross members were originally designed to aid torsional rigidity, but they were removed from the 54mm stand due to time restrictions and their lack of use in a non-thrust vectoring test. However, they are an essential part of the 98mm test stand that will follow this stand.



**Fig. 1: Assembled 54mm Test Stand**

### **B. Vanes and Mounting**

The vane mount's purpose was to hold each jet vane in place throughout the thrust. The vane mount was mounted directly above the nozzle of the motor used. The overall vane mount included three subcomponents include the mounting plate, vane mount, and vanes.

A half-inch steel mounting plate was utilized for its heat resistant properties due to the proximity to the exhaust. Aluminum was chosen for the vane mounts due to its favorable strength-to-weight ratio. The vane mount design consists of a slot shaped like the vane airfoil and two flanges with through holes to mount to the steel mounting plate. Four vane mounts were made to hold each of the vanes and mounted on the steel mounting plate.

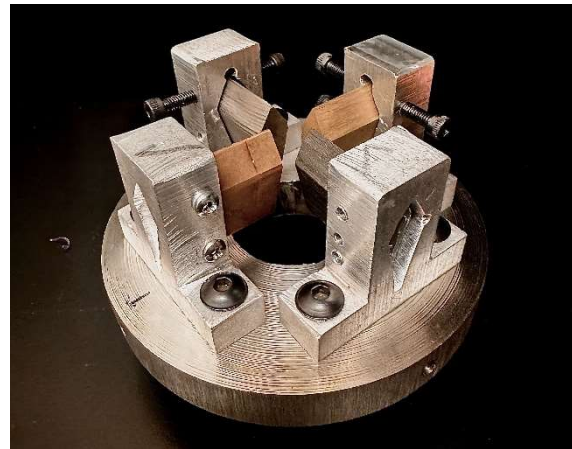
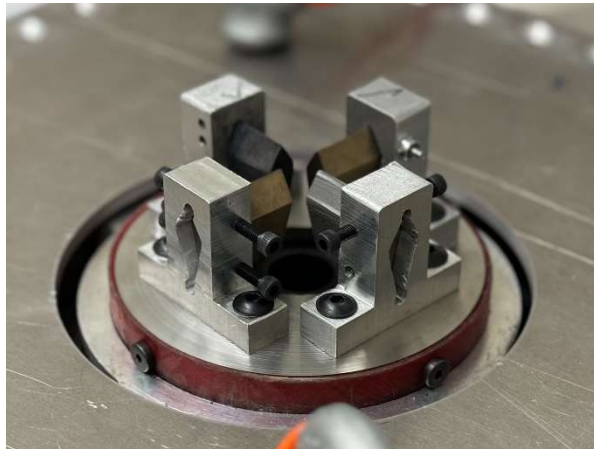


**Fig. 2: Vane Mount Assembly**

The vanes were designed to test material performance under least optimal static fire conditions and design. The vane design incorporated a diamond-shaped airfoil with a 15° wedge angle to maximize material erosion under high-temperature conditions with their leading edge not exceeding 0.3 inches above the nozzle, to facilitate direct exposure to the exhaust gases [5, p.502]

The four jet vane materials tested were 4140 alloy steel, copper-infused tungsten (CIT), tungsten carbide, and graphite. CIT holds precedence in JVTVC systems and similar aerospace applications and is typically used in jet vane-controlled missiles which feature much more aggressive motors with higher aluminum content than the commercial motors used in the test fire [8]. Due to CIT's composite properties of both high hardness and melting temperature, as well as copper's ductility and thermal conductivity (allowing heat to transfer away from the leading edge of the jet vane), it stands out as the standard material for solid propellant jet vane applications (Table 1).

Tungsten carbide was also considered due to its higher operating conditions (the copper in CIT can melt at approximately 1,000°C) [1] and similarly high hardness. Tungsten carbide does, however, suffer from being a brittle material and is too hard to conventionally machine by milling or turning. As a result, tungsten carbide can only be manufactured using a waterjet or a wire EDM machine.

Graphite features the highest operating temperatures [2] of any non-ceramic jet vane candidate material while simultaneously being the cheapest available option. Graphite falls short of any metal options in abrasion resistance and is very brittle. Steel 4140 was selected as a test sample due to its high machineability and its higher toughness compared to other samples. It is also conventionally used in gas turbines which exhibit some similar operational characteristics to jet vanes [3]. Steel 4140 is also a high hardness steel, placing its hardness between tungsten carbide and tungsten copper [4]. For erosion-based wear, erosion itself,  $K$ , can be expressed as [5]:

$$K = f_1(\alpha, n, k) \lambda f \left( \frac{H_a}{H} \right)$$

In which  $H$  is the hardness of the material going under erosion and,  $k$  is a variable that can be described as [5, p. 502]:

$$k = \frac{\phi}{\Omega}$$

In which  $\phi$  denotes the material cutting energy and  $\Omega$  denotes the toughness of the material. These properties made steel 4140 a prominent candidate for testing. However, steel 4140 has a relatively low melting temperature compared to all the samples, and is heat treated to increase its hardness and toughness, therefore being exposed to high temperatures might be detrimental to its structural integrity [4].

**Table 1. Common Properties of Selected Materials for Vanes**

	Steel 4140	Tungsten Carbide (WC)	Copper-infused Tungsten (WCu)	Graphite
Young's Modulus (GPa)	203	600- 686	N/A	4.1- 27.6
Shear Modulus (GPa)	80.0	243	N/A	1.7- 11.5
Density (g/cc)	7.85	15.7	14.3	2.25
Thermal Conductivity (W/m-k)	44.0- 52.0	28-88	190	24
Heat Capacity (J/g-°C)	0.470	0.184- 0.292	0.196	0.7077
Stress at Fracture (MPa)	1020	344	620	13.78-68.9
Strain at Fracture	N/A	0.005- 0.0074	N/A	0.00171- 0.00189
Tensile Strength (MPa)	655	370- 530	585- 654	4.8- 76

Sources: [1,2,46-9]

Initially, the attachment of the vanes to the mounts was to be achieved by drilling through-holes into the vanes, using screws and nuts for securement. However, due to the hardness of tungsten carbide, the available tooling was inadequate. Consequently, set screws were used as an alternative method for securing the vanes, which allowed for precise placement and adjustment. Furthermore, given the brittle nature of graphite, graphite vanes were affixed to the mount using a high-temperature epoxy, avoiding the potential damage to the material when mechanical fastening.

### C. Body Tube & Motor

One of the main purposes of the smaller size of test stand was the ability to characterize the responses of the vanes on the larger, controlled static fire. The most common method of characterizing larger rocket motors is by firing a 54mm motor with the same fuel type and grain geometry. The Cesaroni Technology's M1800-P motor was selected based off burn time, propellant content, and thrust curve shape. This motor uses the propellant formulation known as Blue Streak, which contains a low aluminum content, around 1-3%. This was referenced from the less smoke content from images of Blue Streak motor static fires. The low aluminum content was important as it reduced erosion on the jet vanes due to unburned particle contact and limits slag build up in the nozzle and vanes themselves. To characterize this motor properly, the smaller motor chosen was the Cesaroni Technology J293 motor, also using the Blue Streak propellant. This motor, with a 3.5 second burn time, created a high-powered, continuous burn thrust curve that subjected the vanes to similar conditions that will be felt in the larger static fire.

The body tube, encompassing the internal components and the motor, was a 4" diameter fiberglass tube. This was chosen for its structural stability, ample space for the jet vane mounting configuration, and common use in high powered rocketry for 54mm motors. Because of the motor's length and limited internal components needed for a static fire, the final length of the tube was selected as 10.75".

### D. Bulkhead

The motor bulkhead's primary purpose was to provide a buffer layer between the motor and load cell, aiding in concentrating the thrust force directly to the contact point of the load cell. While the overarching geometry of the part itself is not complex, several interior pocketing and hole patterns were tested alongside varying material selections to gain an understanding of the deflection profile and its spectrum. This profile allows us to visualize the forces acting on crucial areas of the component, giving us the ability to add or remove material at distinct locations.

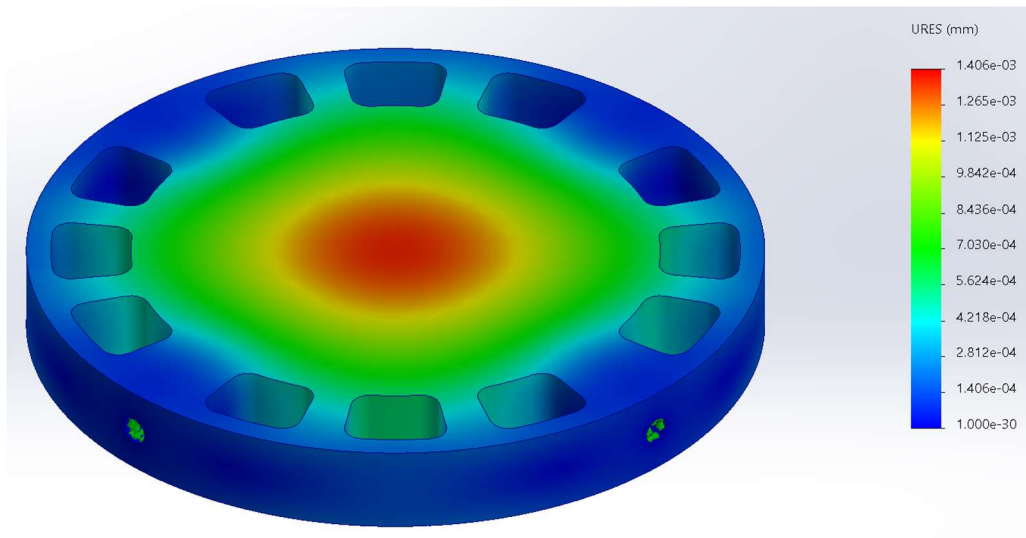


**Fig. 3: Deflection Distribution of Selected Bulkhead Geometry.**

The figure above demonstrates the discussed topological optimization of the bulkhead, which resulted in the removal of large portions of material towards the boundary of the component. We successfully retain a trivial maximum deflection (at the center) even after the significant weight/material cut, proving the effectiveness of the optimization method. Moreover, to refine the design for cost-effectiveness and manufacturability, several common materials were selected and simulated; we primarily examined the resulting deflection and pressure distributions on various aluminum and steels. 6061 aluminum was the final material selection, with minimal deflection (as seen in Figure 1) and low cost, while retaining a quick 2D manufacturing process via a waterjet.

### E. Load Cell Mounts

The load cells collected data on thrust reduction due to vanes and moments. The stand used 3 identical S-Type load cells that could sustain a maximum force of about 2000 N, which was greater than the J293 motor's peak thrust in the z-direction (axial) load cell was placed at the bottom of the body tube assembly. Mounted with an M12x1.75 screw to the base plate, this load cell served as the tool to measure thrust loss caused by the vane interrupting exhaust flow from the nozzle which was one of the main parameters that this test characterized. The x and y load cells were attached 90 degrees apart on an aluminum ring that fit flush around the body tube and placed near the jet vane mount to record lateral force readings due to erosions on the different vanes. Although lateral load cell readings were not used to calculate the thrust curve, they were included to ensure there were no significant lateral loads. These vanes were expected to handle the thrust flow in different ways due to their varying material properties, which would create non-symmetric forces in the x and y-directions that could be measured in tension and compression by the load cells. These x- and y- load cells were mounted to the horizontal steel bars at the top of the test stand and connected to the body tube using an aluminum ring encircling the tube. This way, any x- and y-forces would not be transmitted anywhere apart from the load cells, ensuring maximum efficiency.

### F. Data Acquisition

A National Instruments compactDAQ with an NI 9237 module was used to interface the three load cells with a data acquisition computer, which was configured to sample at 40Hz using a Python script. Each loadcell was calibrated to a  $\pm 50$ -gram accuracy. During each static fire, we recorded data 10 seconds before and after firing to ensure full encapsulation of thrust data as well as changes in zero-thrust weight readings due to motor mass loss. The data was then post-processed to account for weight factors; primarily, the mass change of the motor was linearly interpolated and incorporated into net thrust over burn time, and the weight of all components resting on the load cell (body tube, vane mount, bulkhead, and jet vanes) was added to the net thrust. The remaining offset from zero initial weight readings was likely caused by compression due to mounting tolerancing and was thus subtracted to obtain zero load cell weight before static firing.

## IV. Testing and Results

The static fire revealed conclusive results for both testing parameters. Firstly, vane erosion was found by visual observations and mass calculations before and after both static fires. From the data in Table 2, both tungsten alloys experienced no mass loss, which made them ideal options for the vanes moving forward. Visually, both tungsten alloys had sharp leading edges after the static fires, which proves that the hardness of the materials withstood the slag impacting the vanes at high speeds and temperature without deforming due to thermal and pressure loading. Although the steel alloy and graphite both mechanically withstood both fires, they had too much mass loss to be considered effective for future fires. Due to similar performances of the tungsten alloys, cost and manufacturing time factors had to be considered for the final selection. Although tungsten-copper was up to 5 times more expensive, the machinability and procurement sizes of the material allowed for more complex designs to be made in less time than its tungsten-carbide counterpart. This benefit weighed heavily on the final decision, as student-lead machining is a major constraint on the design process.

**Table 2 - Masses of Individual Jet Vanes Before and After Test fire**

	Copper-Infused Tungsten	Tungsten Carbide	Steel 4140	Graphite
Initial (g)	43.4	45.7	22.7	5.6
After Static Fires (g)	43.4	45.7	22.6	5.3

The second performance parameter measured was the thrust loss. To normalize the raw data, the procedures discussed in Data Acquisition were used. Figure 3 shows the calculated thrust curve after data reduction, and an overlay of the manufacturer’s thrust curve of the J293 motor is also displayed for comparison.

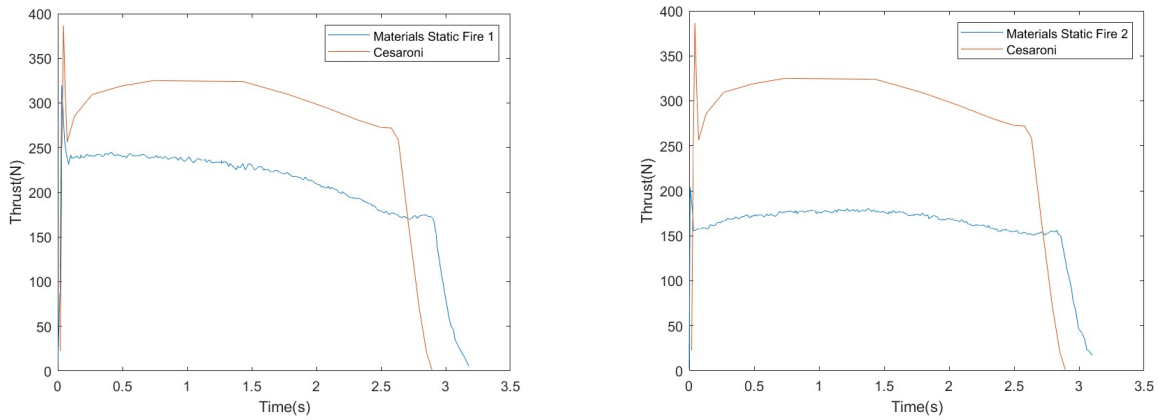


Fig 4: Materials Static Fire 1 and 2 Thrust Curves.



Fig. 5: Vanes after first static fire. Tungsten Carbide, Tungsten Copper, Steel, Graphite



Fig .6: Vanes after second static fire. Tungsten Carbide, Tungsten Copper, Steel, Graphite

## V. Discussion

From the vane performance parameter, the material selected for use was the tungsten-copper alloy. Tungsten-copper provided both the best response to high temperature flow and relative ease of manufacturing to machine complex geometries. Despite its relatively high cost compared to the other materials, the alloy’s material properties proved optimal for jet vanes.

As seen from figure 3, the thrust loss from the jet vane flow was averaged to be around 30%. Possible explanations from this deviation are discussed below:

1. Thrust orientation was likely a small error source in the acquired data. Manufacturer data provides raw thrust data from a laterally oriented motor. The jet vanes static fire was vertically oriented into the ground, which

potentially alters the internal performance of the motor, yielding inaccurate results relative to the manufacturer's original thrust curve. Thus, the actual error may not be exactly as presented in the figures above.

2. External friction from the test stand may have had nontrivial contributions to the observed thrust error. Mainly, friction between the load cell ring (which constrained the body tube from lateral movement) and the body tube was non-negligible. As the body tube was a primary component for load cell readings, this friction may have resulted in an unaccounted upwards force, subtracting from the raw thrust.
3. The loss of axial thrust due to vane deflection is the last source of error in the raw axial thrust readings. Observing the transverse load cell data reveals that the vanes transmitted 10N of force horizontally into the load cells. Though this doesn't account for the full discrepancy between the manufacturer's curve and our axial data, it is an important thrust loss observation.

## **VI. Conclusions**

The development of a motor test stand by the GNC project under the Ramblin' Rocket Club has facilitated a better understanding the design and manufacturing process as well as evaluating thrust, gathering data, determining material properties, and the impacts of testing. The main purpose of this process was to test the various materials of jet vanes to determine what can be used for upcoming TVC projects. This paper also addresses the challenges faced during the development process and what actions were taken to optimize the steps taken.

The research presented in this paper discusses the four materials of jet vanes that were selected to be tested based on multiple factors including the material properties, availability, and manufacturability. The vanes selected play an important role in the thrust direction during flight so the material selected must withstand the extreme temperatures and erosion caused by the motor burn during flight. With the observations from this material static fire, the GNC project aims to use tungsten copper with an optimized vane design in two static fires to test controls software. These three static fires will help the team predict the performance of a TVC system with tungsten copper jet vanes in active stabilization of a rocket.

Looking ahead at the final goal of this GNC project, this first static fire was a step towards gathering data from future experiments to refine the team's JVTVC technology and advance knowledge on active controls. Future tests will include actuation of jet vanes to assess the thrust deflection capabilities during flight. Overall, the culmination of this research represents a significant milestone reached by the GNC team in selecting a material to be used for future thrust vectoring tests and ultimately incorporating it into a rocket.

## References

- [1]"Properties: Tungsten carbide - an overview," AZoM, Accessed March 3, 2024, <https://www.azom.com/properties.aspx?ArticleID=1203>.
- [2]"Graphite, Carbon, C," MatWeb, Accessed March 3, 2024, <https://www.matweb.com/search/DataSheet.aspx?MatGUID=3f64b985402445c0a5af911135909344>.
- [3]Rahaim, Christopher, et al., "Jet Vane Thrust Vector Control - a Design Effort," 32nd Joint Propulsion Conference and Exhibit, July 1, 1996, doi:10.2514/6.1996-2904.
- [4]"AISI 4140," MatWeb, Accessed March 3, 2024, [www.matweb.com/search/DataSheet.aspx?MatGUID=8b43d8b59e4140b88ef666336ba7371a&ckck=1](http://www.matweb.com/search/DataSheet.aspx?MatGUID=8b43d8b59e4140b88ef666336ba7371a&ckck=1).
- [5]Magnée, A., "Generalized Law of Erosion: Application to Various Alloys and Intermetallics," *Wear*, Vol. 181–183, March 1995, pp. 500–510, doi:10.1016/0043-1648(94)07072-5.
- [6]"Data sheet tungsten-copper (WCU)," WHS Sondermetalle, Accessed March 3, 2024, <https://www.whs-sondermetalle.de/images/pdf/WCu-Tungsten-Copper.pdf>.
- [7]"Tungsten Carbide, WC," MatWeb, Accessed March 3, 2024, <https://www.matweb.com/search/DataSheet.aspx?MatGUID=e68b647b86104478a32012cbbd5ad3ea>.
- [8]"Tungsten copper: EDM electrode, Heat sink: W cu properties and applications," Chemetal USA, Accessed March 3, 2024, <https://www.chemetalusa.com/copper-tungsten/>.
- [9]"4140 low-alloy steel," Desktop Metal, Accessed March 3, 2024, <https://www.desktopmetal.com/uploads/SPJ-SPC-MDS-4140-210602.c.pdf>.